Kinetics of Solvent Diffusion and Swelling in a Model Elastomeric System

Ken A. Mazich,[†] **Giuseppe Rossi,*** **and Cindy A. Smith**

Scientific Research Laboratory, Room E-3172, Ford Motor Company, P.O. Box 2053,
Mail Drop 3198, Dearborn, Michigan 48121-2053

Received July 13, 1992; Revised Manuscript Received September 9, 1992

ABSTRACT: We measure solvent uptake (and loss) taking place as toluene diffuses in and out of cross-linked polyisoprene spheres. We analyze our experimental data using a theoretical description of the swelling process recently put forward by two of us and use these data to test the physical assumptions at the basis of our description. We find that even though this system displays features which are commonly regarded as signature for anomalous or "non-Fickian" behavior (sigmoidal uptake), a correct use of Fick's law accounts for the evolution of the system within the limits of our experimental error. Our data analysis allows us to obtain information on the dependence of the diffusion coefficient on concentration.

I. Introduction

Studies of the diffusion of solvent in a polymeric system have uncovered a variety of different situations and regimes.[1] The specific features observed during the diffusion process are determined to a large extent by the state of aggregation of the polymer. Indeed, in certain classes of systems, diffusion of penetrant is accompanied by a change of the state of aggregation of the polymeric system. For example, plasticization, e.g., lowering of the glass transition temperature, takes place in polymeric glasses, and a sharp front divides the plasticized from the unplasticized region.[2,3]

Diffusion of solvent in a cross-linked rubber or gel represents a special case: in the case of good solvent, significant swelling (often up to many times the size of the dry sample) may occur. In a number of situations swelling is accompanied by formation of wrinkles or patterns on the surface of the sample and in some instances the sample has been observed to fracture.[4–7]

Early studies on these systems were directed at measuring sorption (and desorption) curves both in the case of elastomers put in contact with solvent vapor[8–10] and for situations where the polymeric material is actually immersed in liquid solvent.[11] For the latter case, interferometric measurements aimed at determining the form of the solvent concentration profile as a function of time were also performed.[12–14] These results were analyzed using the ordinary diffusion equation; neither the movement (due to swelling) of the boundaries of the polymer occupied region nor the effect of constraints applied to the elastomer were taken into account. We believe that this inappropriate analysis is responsible for some of the puzzling conclusions reached in these works and in particular for the unusual concentration dependence of the mutual diffusion coefficient obtained in refs 12 and 14; these authors find mutual diffusion coefficients for benzene and toluene in natural rubber which exhibit a maximum at intermediate (≈ 0.5) solvent concentrations. Even an unusual dependence of the diffusion coefficient on concentration is insufficient to explain a second puzzling feature reported for the first time in ref 11 and confirmed by more recent sorption studies:[15] the sorption curves for the solvent uptake as a function of $t^{1/2}$ in a number of simple polymer solvent systems (natural rubber in *n*-decane, natural rubber in toluene) exhibit sigmoidal (also referred to as S-shaped) behavior. Such behavior has been ordinarily regarded as a signature of anomalous or "non-Fickian" effects;[16] however, it is difficult to accept that such effects may be relevant in networks which are not very tightly cross-linked and are well above the glass transition temperature.

In the last decade, there have been attempts to provide a more complete theoretical description of the kinetics of the swelling process based on the notion of "cooperative" diffusion.[17,18] These works appear to be flawed by internal inconsistencies.[19] Furthermore, the experimental evidence presented tests only very general qualitative features, e.g., the fact that swelling time is proportional to the square of the sample linear dimensions and that the approach to equilibrium is exponential; such experiments do not constitute a test for the details of the theoretical treatment.

Recently two of us put forward a new description of the kinetics of swelling for cross-linked polymer networks;[20,21] this description is based on the same simple physical assumption on which the usual mathematical description of diffusion in a porous medium is based. Namely we assume that Fick's law is valid, i.e., that the flux (of polymer or solvent) is proportional to the local gradient of concentration. The proportionality constant is the mutual diffusion coefficient D_M and can depend on the local state variables (concentration, temperature, etc.). We also assume that at the boundary of the polymer occupied region equilibrium is achieved as soon as the polymeric sample comes in contact with the solvent. On the basis of these assumptions we find equations which account in a consistent way for the fact that polymeric material is displaced as solvent moves in, i.e., for the presence of moving boundaries. We have written equations both for one dimension and for the spherically symmetric three-dimensional problem; however, we have been so far unable to extend our treatment to a general three-dimensional geometry.

In this paper we revisit a simple rubber–solvent system, polyisoprene spheres swelling in toluene, and treat our experimental data using the theoretical methods put forward in refs 20 and 21. It is important to realize that without a proper macroscopic theoretical description of the swelling process, a correct determination of the diffusion coefficient and its concentration dependence is not possible; this is the information needed to shed light on the microscopic processes taking place as solvent mixes with the polymer chains in the network. This paper is organized as follows: In the rest of this section we briefly

---

[†] Present address: Dow Corning Corporation, Analytical Research Department, Midland, MI 48686-0994.

0024-9297/92/2225-6929$03.00/0

summarize the theoretical approach of refs 20 and 21. Our experimental results are described in the next section. The last section contains a detailed comparison between these results and our theoretical predictions.

In refs 20 and 21 we found that since polymer is displaced as solvent diffuses in the network, it is convenient to write the equations for the concentration profiles in lagrangian coordinates. For example, for one dimension we found

$$\frac{\partial\phi_{\mathrm{R}}(x_0,t)}{\partial t} = \phi_{\mathrm{R}}^{2}(x_0,t)\left(D_{\mathrm{M}}(\phi_{\mathrm{R}})\frac{\partial^2\phi_{\mathrm{R}}(x_0,t)}{\partial x_0^{2}} + \frac{\partial D_{\mathrm{M}}(\phi_{\mathrm{R}})}{\partial\phi_{\mathrm{R}}}\left(\frac{\partial\phi_{\mathrm{R}}(x_0,t)}{\partial x_0}\right)^2\right) \quad (1)$$

This equation describes the time evolution of the polymer concentration $\phi_{\mathrm{R}}(x_0,t)$ in the volume element of network which was located in $x = x_0$ at time $t = 0$. At a later time, t, this volume element is displaced to $x = x_{\mathrm{R}}$ where

$$x_{\mathrm{R}}(x_0,t) = \int_0^{x_0}\frac{\mathrm{d}x_0}{\phi_{\mathrm{R}}(x_0,t)} \quad (2)$$

Therefore solving eq 1 and transforming back to the laboratory frame using eq 2 allows us to obtain the polymer concentration profiles. These equations refer to a model situation where both the density of the polymer and solvent are fixed and equal to 1, so that concentrations and volume fractions coincide; the solvent and polymer concentrations obey

$$\phi_{\mathrm{S}}(x,t) + \phi_{\mathrm{R}}(x,t) = 1 \quad (3)$$

everywhere throughout the swelling process.

The analog of eq 1 for a spherically symmetric three-dimensional situation is

$$\frac{\partial\phi_{\mathrm{R}}}{\partial t} = \frac{2r_{\mathrm{R}}\phi_{\mathrm{R}}D_{\mathrm{M}}(\phi_{\mathrm{R}})}{r_0^{2}}\left(2-\frac{r_{\mathrm{R}}^{3}\phi_{\mathrm{R}}}{r_0^{3}}\right)\left(\frac{\partial\phi_{\mathrm{R}}}{\partial r_0}\right) + \frac{r_{\mathrm{R}}^{4}\phi_{\mathrm{R}}^{2}}{r_0^{4}}\left(\frac{\partial(D_{\mathrm{M}}(\phi_{\mathrm{R}}))}{\partial\phi_{\mathrm{R}}}\left(\frac{\partial\phi_{\mathrm{R}}}{\partial r_0}\right)^2 + D_{\mathrm{M}}(\phi_{\mathrm{R}})\frac{\partial^2\phi_{\mathrm{R}}}{\partial r_0^{2}}\right) \quad (4)$$

Again this equation describes the evolution in time of the polymer concentration $\phi(r_0,t)$ in the spherical shell which was located at $r = r_0$ at time $t = 0$. At a later time, t, the radial position of this shell is $r = r_{\mathrm{R}}(r_0,t)$ where

$$r_{\mathrm{R}}^{3}(r_0,t) = 3\int_0^{r_0}\frac{r_0^{2}\,\mathrm{d}r_0}{\phi_{\mathrm{R}}(r_0,t)} \quad (5)$$

The value of the network equilibrium swelling concentration $\Phi_{\mathrm{R}}^{(\mathrm{eq})}$ is used as a boundary condition to solve eqs (2) and (4). Microscopic information on the specific polymer solvent interaction (Flory's χ parameter) and on the structure of the network (number of monomers between cross-links) enters our treatment through the boundary conditions. If $\Phi_{\mathrm{R}}^{(\mathrm{eq})}$ and the form $D_{\mathrm{M}}(\phi_{\mathrm{R}})$ of the mutual diffusion coefficient are known, eqs 2 and 3 and 4 and 5 completely determine the time evolution of the solvent concentration profiles, and the solvent uptake or loss $M(t)$ can be obtained by an appropriate quadrature. For the spherical geometry considered below, $M(t)$ is defined by

$$M(t) = |(4\pi/3)\cdot(r_{\mathrm{R}}^{3}(a_0,t) - a_0^{3})| \quad (6)$$

where a_0 is the initial sphere radius.

Two new qualitative features which were not predicted by previous theoretical treatments are found in our description for the case of high equilibrium solvent concentrations. These are (see ref 21 for details): (i) the fact that deswelling takes place faster than swelling at least at short times (if the diffusion coefficient increases markedly with solvent concentration the sorption and desorption curves may cross each other at some finite time); (ii) the sigmoidal character of the solvent uptake (sorption) curve in the case of spherical geometry, this feature is found even for a constant D_{M}, but becomes more pronounced if D_{M} increases with solvent concentration. Both of these qualitative features are illustrated in Figure 1 as they occur for a constant $D_{\mathrm{M}} = 1$ and for $\Phi_{\mathrm{R}}^{(\mathrm{eq})} = 0.156$ in the case of a sphere of initial unit radius. These curves were found by solving numerically eq 4 using an implicit finite difference algorithm.[22]

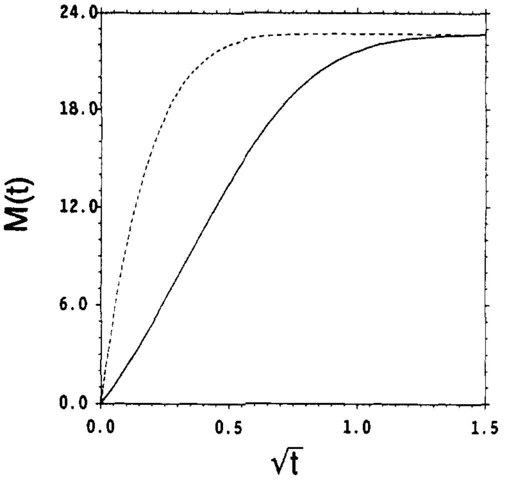

Figure 1. Theoretical predictions for solvent uptake (solid curve) and loss (broken curve) $M(t)$ vs $t^{1/2}$ in the case of a sphere of initial unit radius swelling to a final equilibrium concentration $\Phi_{\mathrm{R}}^{(\mathrm{eq})} = 0.156$. We used $D_{\mathrm{M}} = 1$.

II. Experimental Section

Samples of commercial *cis*-1,4-polyisoprene (Natsyn 2200) supplied by Goodyear were mixed with different amounts, 1–5 phr (parts per hundred rubber, by weight) of dicumyl peroxide (Varox DCP-R) supplied by R.T. Vanderbilt, Inc., on a small two-roll mill at room temperature. Pieces of material prepared in this way were then used to fill the two hemispheres of a spherical steel mold and were press cured for 90 min at 150 °C.

The small rubber spheres obtained in this way (radius $a_0 \approx 6.2$ mm[23]) were immersed in a 2 in. × 2 in. × 2 in. optical cell filled with toluene and were allowed to swell to their equilibrium concentration. Images of the spheres were acquired during the swelling process, and the time evolution of the radius (and hence the volume) was obtained in this way. In a number of cases we did double check our results with the aid of a traveling microscope. No significant surface pattern formation of the kind described in refs 4–7 was observed during the swelling process and the shape of the specimens remained spherical throughout the process; the error bars shown in Figures 5, 6, and 7 correspond to standard deviation on the value of the spheres radii obtained from our images.

After the spheres had reached their final equilibrium concentration in toluene, some of the spheres were deswollen in air and some were deswollen by immersion in methanol. We experienced a number of problems with the deswelling experiment in air. The most tightly cross-linked specimen (5 phr) did undergo large scale fracture shortly (a few minutes) after deswelling began. During deswelling in air of the remaining specimens, significant deviations from a regular spherical shape were observed in a number of instances (especially at short times and in correspondence to the part of the surface on which the sphere was resting). Even in those cases where only minor deviations from a spherical shape were observed, we do not feel that we had the experiment under control; initially (first couple of hours) due to pressure from toluene diffusing out between the sphere and its support,

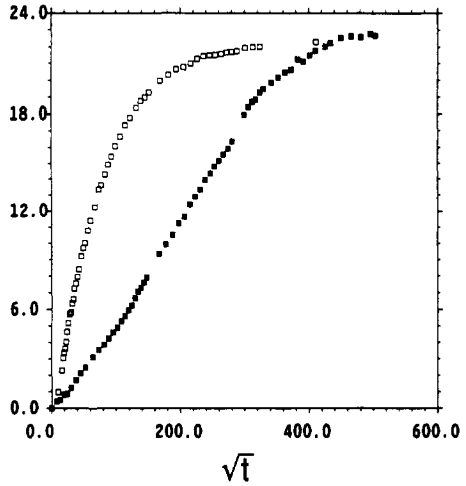

Figure 2. Experimental results for solvent uptake (solid symbols) and loss (open symbols) $M(t)$ vs $t^{1/2}$ for a sphere which was swollen in toluene to a final equilibrium concentration $\Phi_R^{(eq)} = 0.156$ and subsequently deswollen in methanol. See text for the normalization of $M(t)$.

the sphere kept moving in a way reminiscent of dry ice left on a table. Nevertheless, we report an example of desorption curve obtained under these conditions in Figure 4.

We did not experience any such problems when the swollen spheres were immersed in methanol. However, the data obtained for deswelling in methanol are difficult to interpret. This is because deswelling results from the combined effect of toluene diffusing out of the polymer occupied region and methanol diffusing in it; this second effect may be sizable, especially initially, when the polymer occupied region is mostly occupied by toluene. The swollen polyisoprene spheres were nearly transparent when they were first immersed in methanol, but late in the process of deswelling, they became milky white. We also observed this change in color for dry polyisoprene spheres immersed in methanol (in this latter case the final uptake is of the order of a few percent).

Typical data for a swelling–deswelling cycle are shown in Figure 2. In this particular instance the ratio of the final swollen equilibrium volume V_F to the initial volume V_0 was $V_F/V_0 = 6.41$. The initial radius of the sphere was $a_0 = 6.22 \pm 0.01$ mm. These deswelling data refer to immersion of the swollen sphere in methanol. We plot solvent uptake (loss) vs $t^{1/2}$; time is measured in seconds (note that the time range covered in Figure 2 is 100 h). The data for solvent uptake (loss) are normalized so that the initial radius of the sphere is the unit of length: i.e., we plot $M(t) = 4\pi(V(t) - V_0)/3V_0$ (uptake) and $M(t) = 4\pi(V_F - V(t))/3V_0$ (loss). At the end of the swelling–deswelling cycle we found that the final volume was about 1.08 times the initial volume V_0: this increase in volume is due mostly to methanol uptake and partly to the fact that, owing to the finite size of our optical cell, the sphere is not in contact with an infinite methanol reservoir; therefore, some residual toluene remains in the polymer occupied region. It should be clear already from a comparison of Figures 1 and 2 that the qualitative predictions obtained from our treatment are confirmed by our experimental results.[24] Note that, since we used the naive assumption of a constant diffusion coefficient, the only experimental parameter entering the curves of Figure 1 is the final equilibrium concentration $\Phi_R^{(eq)}$.

Figure 3 contains our sorption results; these data cover the range of swelling ratios from $V_F/V_0 = 3.55$ to $V_F/V_0 = 6.41$. On the log–log plot of Figure 3, a multiplicative constant entering the diffusion coefficient corresponds to an overall translation of the sorption curve parallel to the t axis. Likewise, due to our choice of normalization for the solvent uptake ($M(t) = 4\pi(V(t) - V_0)/3V_0$), the sorption curves for two spheres made of the same cross-linked material but having different initial radii a_1 and a_2 would be translated with respect to each other by an amount 2 log (a_1/a_2) parallel to the t axis. Figure 4 contains some of our results for desorption. The two upper data sets refer to desorption in methanol. An example of desorption in air is also shown; in this case only minor deviations from spherical shape were observed.

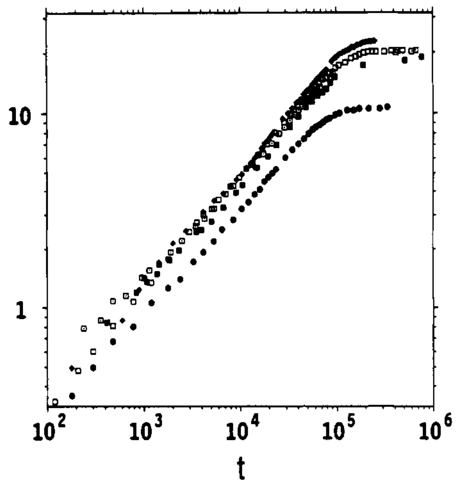

Figure 3. Experimental results for solvent uptake $M(t)$ vs t for spheres obtained from material prepared with different degrees of cross-linking.

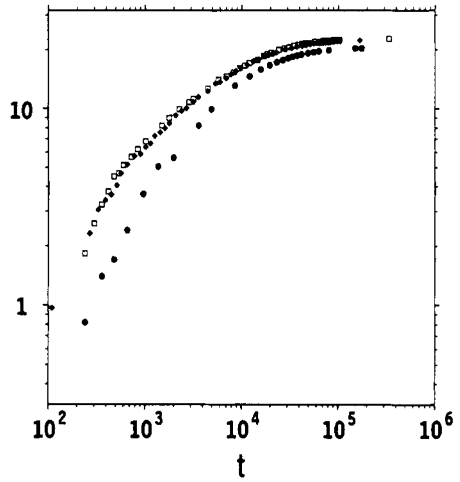

Figure 4. Experimental results for solvent loss $M(t)$ vs t for spheres deswollen in methanol (squares and diamonds) and in air (circles).

III. Discussion

As pointed out in the previous section, the new qualitative features predicted by our theoretical description are confirmed by the experimental data. In this section we attempt a more detailed quantitative comparison between our predictions and the data for sorption and desorption shown above. Our aim is to test the assumptions of our theoretical approach and to obtain information on the concentration dependence of the mutual diffusion coefficient D_M. We chose to fit our sorption data with the following form for D_M (ϕ_R):

$$D_M(\phi_R) = D_0 e^{\alpha(1-\phi_R)} \qquad (7)$$

Although there seems to be no compelling reason to justify the exponential dependence on solvent concentration, this form has been used extensively in the literature.[10,25]

Once the form (7) has been agreed upon, three phenomenological parameters, i.e., D_0, α, and the equilibrium concentration $\Phi_R^{(eq)}$, enter our theoretical description. We can fix $\Phi_R^{(eq)}$ using the last data point in our sorption curves. As noted above D_0 fixes the scale of time, and in a log–log plot changing D_0 corresponds to a parallel translation of the sorption curve; on such a plot α is the only parameter which can be tuned to change the shape of the curves.

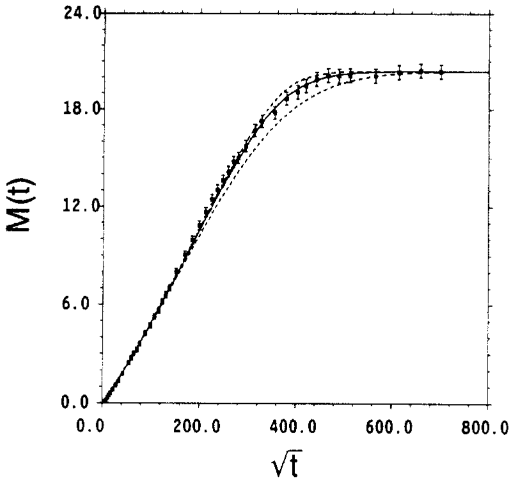

Figure 5. Experimental results for a sorption uptake experiment are compared to our theoretical prediction corresponding to the value of $\Phi_R^{(eq)}$ given by the final data point. We show predictions for $\alpha = 0.0$ (lower broken curve), $\alpha = 3.0$ (solid curve), and $\alpha = 6.0$ (upper broken curve).

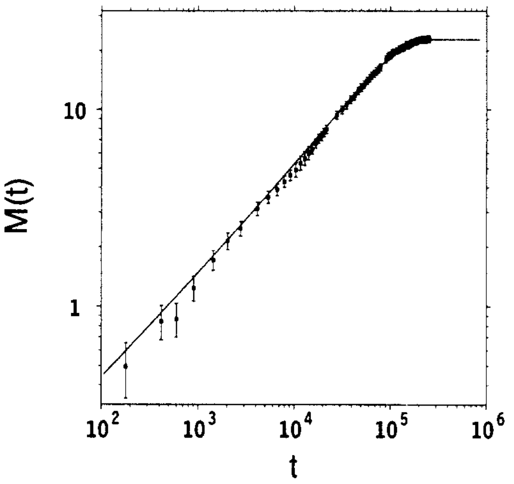

Figure 6. Comparison between the experimental sorption data reported in Figure 2 and our prediction obtained using $\alpha = 3.0$ and $D_0 = 2.3 \times 10^{-7}$ cm^2/s.

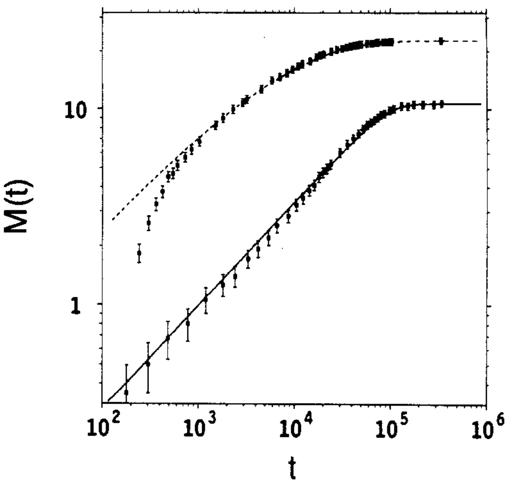

Figure 7. The lower set of data shows a comparison between sorption data obtained for our most tightly cross-linked specimen and our prediction obtained by using $\alpha = 3.0$ and $D_0 = 3.1 \times 10^{-7}$ cm^2/s. The upper set of data shows the result of our attempt to match data for deswelling in methanol with the solution of our equations; we used $\alpha = 3.0$ and $D_0 = 4.9 \times 10^{-7}$ cm^2/s.

In Figure 5 we show our procedure to obtain information on the concentration dependence of D_M. Here we are working with the data shown as unfilled squares in Figure 3; in this case $\Phi_R^{(eq)} = 0.171$. Corresponding to this value of $\Phi_R^{(eq)}$, we plot predictions for the sorption curves obtained from our equations for $\alpha = 0.0$, $\alpha = 3.0$, and $\alpha = 6.0$; in each case D_0 is chosen so as to match as closely as possible the initial sorption data.[26] It should be clear that our results for the sorption curves are very insensitive to the value of α; it is not possible to fine tune α so as to match any given experimental shape. Therefore, a comparison with the experimental sorption curves constitutes a severe test for our predictions. However, the insensitivity also means that it is difficult to discriminate between different values of α. The data shown in Figure 5 appear to rule out a constant diffusion coefficient ($\alpha = 0.0$). On the basis of these data and of similar results obtained for the other sorption curves, we tentatively take $\alpha = 3.0$. We note however, that on the basis of this same procedure, one would have been equally justified in choosing for example $\alpha = 4.0$.

Using $\alpha = 3.0$ and $D_0 = 2.3 \times 10^{-7}$ cm^2/s, we have been able to obtain satisfactory agreement (an example is shown in Figure 6) between theoretical results and experimental data for all of our sorption curves except the one for the most tightly cross-linked sphere. In this case, if we insist on the choice $\alpha = 3.0$, the value $D_0 = 3.1 \times 10^{-7}$ cm^2/s seems to be appropriate; the result is shown in Figure 7 (solid curve).[27] In Figure 7 we also show an attempt to match our data for deswelling in methanol (broken curve). In this case we are clearly unable to capture satisfactorily the initial desorption data; as we have remarked above, we expect three component diffusion to be important in this regime. The theoretical curve shown in the figure corresponds to $\alpha = 3.0$ and to an "effective" $D_0 = 4.9 \times 10^{-7}$ cm^2/s. It is not surprising, in view of the experimental problems described in the previous section, that we have not been able to match in a satisfactory way theoretical desorption curves with our data for deswelling in air.

In view of these results, it seems fair to state that the theoretical description of refs 20 and 21 not only captures the qualitative features of the sorption–desorption process for the model system that we have examined but also, in the case of sorption, can afford detailed quantitative predictions. Indeed the data presented in this paper appear to provide provisional confirmation for the working hypotheses at the basis of the theoretical treatment of refs 20 and 21; e.g., they indicate that, for the simple model system considered here, Fick's law of diffusion is valid (at least at low cross-linking levels[27]) and that it is sensible to assume that equilibrium is reached at the boundary of the polymer occupied region as soon as polymer is put in contact with solvent.

More data are needed to fully test our description. In particular, sorption and desorption experiments in vapor (e.g., at low final solvent concentration) on spherical specimens would provide information in a regime where our description has not been tested thus far. Such experiments could give more data on the dependence on concentration of the diffusion coefficient and could shed light on the importance of the geometrical shape of the specimen on the form of the sorption curves. We suspect that the desorption experiment may be less worrisome in this situation. Experiments with different polymer–solvent systems are also needed to test whether the qualitative features reported in this paper are indeed general, as we expect from our treatment.

Acknowledgment. We wish to acknowledge useful conversations with Jim Anderson, George Mozurkewich and Phil Pincus. We are indebted to Fred Oblinger for helping us in the design of the mold and for preparing some of the samples.

References and Notes

(1) Crank, J.; Park, G. S. *Diffusion in Polymers*; Academic Press: New York, 1968. See also: Errede, L. A. *Adv. Polym. Sci.* **1991**, *99*, 1, and references therein.

(2) Hui, C. Y.; Wu, K. C.; Lasky, R. C.; Kramer, E. J. *J. Appl. Phys.* **1987**, *61*, 5129 and 5137.

(3) Alfrey, T.; Gurnee, E. F.; Lloyd, W. G. *J. Polym. Sci., Part C* **1966**, *12*, 249.

(4) Southern E.; Thomas, A. G. *J. Polym. Sci.* **1965**, *A3*, 611.

(5) Patrikeev, G. A.; Chong, B.; Kondratov, A. P. *Vysokomol. Soedin., Ser. B* **1984**, *26*, 485.

(6) Tanaka, T. *Physica* **1986**, *140A*, 261. Tanaka, T.; Sun, S. T.; Hirokawa, Y.; Katayama, S.; Kucera, J.; Hirose, Y.; Amiya, T. *Nature* **1987**, *325*, 796.

(7) Rossi, G.; Smith C. A.; Mazich, K. A. Unpublished report SR-92-101.

(8) Prager, S.; Long, F. A. *J. Am. Chem. Soc.* **1951**, *73*, 4072.

(9) Hayes, M. J.; Park, G. S. *Trans. Faraday Soc.* **1955**, *51*, 1134.

(10) van Amerongen, G. J. *Rubber Chem. Technol.* **1964**, *37*, 1065.

(11) Southern, E.; Thomas, A. G. *Trans. Faraday Soc.* **1967**, *63*, 1913.

(12) Hayes, M. J.; Park, G. S. *Trans. Faraday Soc.* **1956**, *52*, 949.

(13) Buckley, D. J.; Berger, M.; Poller, D. *J. Polym. Sci., Polym. Phys. Ed.* **1962**, *56*, 163. Buckley, D. J.; Berger, M. *J. Polym. Sci., Polym. Phys. Ed.* **1962**, *56*, 175.

(14) Mozisek, M. *Makromol. Chem.* **1970**, *136*, 87.

(15) Waksman, L. S.; Schneider, N. S.; Sung, N. H. In *Barrier Polymers and Structures*; Koros, W. T., Ed.; American Chemical Society: Washington, DC, 1990.

(16) Fujita, H. *Fortschr. Hochpolym.-Forsch.* **1961**, *3*, 1.

(17) Tanaka, T.; Fillmore, D. J. *J. Chem. Phys.* **1979**, *70*, 1214.

(18) Peters, A.; Candau, S. J. *Macromolecules* **1986**, *19*, 1952. Peters A.; Candau, S. J. *Macromolecules* **1988**, *21*, 2278.

(19) In refs 17 and 18 the equation for the radial component of the displacement vector in spherical coordinates is not consistent with the equation for the vector itself, from which it is purportedly derived (the divergence of a gradient is confused with the gradient of a divergence). The notion of a cooperative diffusion coefficient and its relation with the gel elastic moduli given by these authors are based on this flawed derivation.

(20) Rossi, G.; Mazich, K. A. *Phys. Rev.* **1991**, *A44*, R4793.

(21) Rossi, G.; Mazich, K. A. Submitted to *Phys. Rev. A*.

(22) Ames, W. F. *Numerical Methods for Partial Differential Equations*; Academic Press: New York, 1977.

(23) Since the time needed to reach equilibrium is proportional to the square of the radius of the spheres, using smaller spheres makes the experiment less time-consuming. We recently obtained some preliminary data with spheres of initial radius $a_0 \approx 4.7$ mm. These data are consistent with those presented in the text.

(24) To our knowledge the fact that deswelling takes place faster than swelling in the case of high equilibrium solvent concentration has not previously been reported. On the basis of our equations, we expect this to be a general phenomenon. The desorption curves found in the literature refer to low equilibrium concentration. Our equations predict that in this case desorption will be slower than sorption if D_M increases sufficiently fast with solvent concentration; see ref 21 for details.

(25) Thomas, N. L.; Windle, A. H. *Polymer* **1982**, *23*, 529. Herman, M. F.; Edwards, S. F. *Macromolecules* **1990**, *23*, 3662.

(26) The curves of Figure 5 correspond to $D_0 = 1.6 \times 10^{-6}$ cm^2/s for $\alpha = 0.0$, $D_0 = 2.3 \times 10^{-7}$ cm^2/s for $\alpha = 3.0$, and $D_0 = 2.9 \times 10^{-8}$ cm^2/s for $\alpha = 6.0$.

(27) An equally good match could have been obtained by keeping D_0 unchanged and choosing a slightly larger α. In either case, the result of these fits is that the diffusion coefficient for the most tightly cross-linked rubber is larger than that obtained for the more loosely cross-linked specimens: naively one would expect the diffusion coefficient to decrease as the network gets tighter. Our result may be an indication of the fact that elastic effects, which are not explicitly accounted for in our theoretical treatment, begin to play a role at these levels of cross-linking. Still, in view of the agreement (see Figure 7, lower curve) between experimental results and theoretical predictions, it seems that in our treatment elastic contributions to the flux are largely accounted for in an effective way by the new value of D_0 (or α).